SSRG International Journal of Mechanical Engineering
ISSN: 2348-8360/ https://doi.org/10.14445/23488360/IJME-V11I10P101

Volume 11 Issue 10, 1-7, October 2024

Original Article

Effects of Blast Furnace Slag Particles on Microstructure and Mechanical Properties of Al-4Mg Alloy Manufactured by Stir Casting

Konda Sreedevi[1], Koonja Ramji[2], M. Gopi Krishna[3]

[1,2]*Mechanical Engineering, Andhra University College of Engineeringg, Andhra Pradesh, India.*
[3]*Mechanical Engineering, University College of Engineering, Acharya Nagarjuna University, Andhra Pradesh, India.*

[3]*Corresponding Author : mgopi.anu@gmail.com*

Received: 01 August 2024 Revised: 02 September 2024 Accepted: 02 October 2024 Published: 30 October 2024

Abstract *- The study significantly contributes to the knowledge of utilizing blast furnace slag as a reinforcement material in Al-4Mg alloys, highlighting its potential for various applications in the automotive, aerospace, and automotive industries by successfully fabricating composites with varying weight percentages of slag. The thorough investigation of grain structure changes and uniform particle distribution through advanced microscopy techniques provides valuable insights into the reinforcement mechanisms. The observed improvements in mechanical properties, particularly in hardness, density, Young's modulus, compressive strength, and tensile strength, with the addition of 5% slag reinforcement, underscore the practical significance of these composites. This finding indicates that Al-4Mg alloy composites with blast furnace slag can potentially offer lightweight yet high-strength materials suitable for demanding applications in the automotive and aerospace industries. Overall, the study's results not only demonstrate the enhanced performance of the composites but also highlight the eco-friendliness and cost-effectiveness of using blast furnace slag as a reinforcement material.*

Keywords *- Al-Mg composites, Stir casting, Mechanical properties, and characterization.*

1. Introduction

In the current decade, a significant amount of research has been dedicated to improving automobile performance by exploring alternative materials that are both efficient and cost-effective. These alternatives include cast iron, polymers, other aluminum alloys, and composites as potential replacements for Al-Mg materials [1-4]. The selection of materials is based on their functionality, cost, and eco-friendliness, which are crucial factors in achieving improved automotive performance. One key aspect in material selection is the size, type, and weight percentage of the reinforcement, as their interactions with the matrix play a vital role in determining the mechanical properties of the final product. Researchers have observed that the use of reinforcement can lead to benefits such as increased melting point, thermal stability, hardness, and strength [5-9]. Various manufacturing processes, including powder metallurgy composites, powder sintering, spray deposition, and stir casting, have been explored for creating composites [10-11]. Among these methods, stir casting stands out as a favorable option due to its low cost and rapid production rate. Stir casting involves using stirring techniques to evenly disperse reinforcements in a liquid state [12]. However, despite the progress in using different reinforcement materials and manufacturing processes, there is still a research gap in exploring the utilization of specific waste products as reinforcement in stir-cast composites. This work aims to address this research gap by using blast furnace slag as reinforcement in stir-cast composites. Blast furnace slag is an industrial waste product with the potential to enhance the mechanical properties of composites. By investigating the properties of blast furnace slag-reinforced composites, the researchers hope to explore a novel approach to improve the performance of automobiles while also utilizing waste materials, thus contributing to the development of eco-friendly and cost-effective automotive materials.

In summary, the novelty of this work lies in the use of blast furnace slag as a reinforcement material in stir-cast composites for automobile applications. This research addresses the current literature's research gap by exploring an innovative and sustainable approach to enhance the mechanical properties of automotive materials. Argon gas is continuously impinged around the melt to prevent oxidation. The BF Slag particles enhance the strength properties and improve wear resistance. The research results obtained in this study were critically analyzed by comparing them with the existing literature on alternative materials for improving automobile performance. The mechanical properties of the

blast furnace slag-reinforced composites were evaluated and contrasted with those reported in the literature for other reinforcement materials. It was found that the use of blast furnace slag as a reinforcement material led to noticeable improvements in hardness, strength, and toughness, which were compared favorably with other studied materials.

2. Materials and Methods

2.1. Materials

Commercially available elemental Aluminium and magnesium metals were brought in ingot form, supplied by Venuka Engineering Pvt Ltd Hyderabad. In this work, blast furnace slag particles of size 53µm proposed to reinforce into an Al-4 Mg alloy matrix. The reinforced particles were collected from RINL, Steel Plant Visakhapatnam; sieve analysis was performed to identify the particle size. Figure 1 shows the microstructure of slag particles, which have a flaky structure. The elements of blast slag particles are large amounts of Calcium Oxide (CaO), Silica (SiO_2), Alumina (Al_2O_3), and Magnesium oxide (MgO).

Table 1. Elemental chemical composition of BF slag particles

Ele	SiO_2	Al_2O_3	CaO	MgO	Fe_2O_3	K_2O	Na_2O_3
Wt%	33.7	13.11	42	7.4	0.51	0.3	0.16

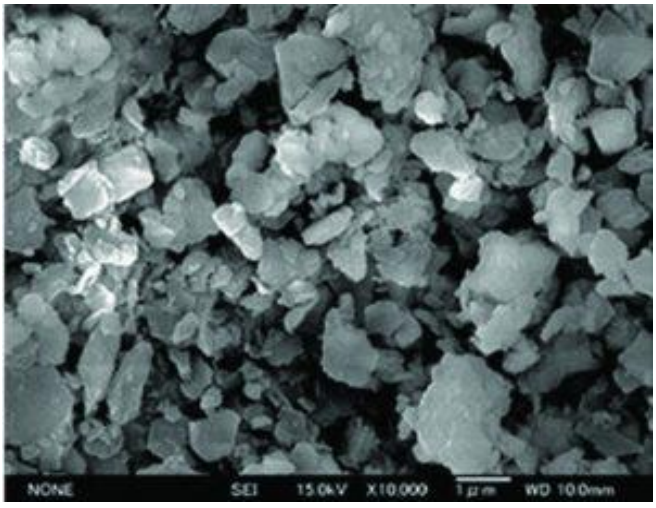

Fig. 1 Microstructural image of BF slag reinforcements

2.2. Binary Alloy Preparation

Aluminium ingots, provided by Hindalco, were first weighed and placed in a clay-graphite crucible. The crucible was then positioned inside a furnace, with the temperature set to 700°C.

To prevent the aluminium from oxidizing, a small quantity of coverall powder (Hexachloroethane), amounting to about 0.1% of the total metal weight, was added at the start of the melting process. Once the aluminium had completely melted, a pre-weighed magnesium piece (4% of the aluminium weight), wrapped in aluminium foil, was carefully lowered into the molten aluminium using a cup-shaped graphite dipper. The magnesium piece was submerged to the bottom to ensure full dissolution and argon gas was directed around the melt to prevent oxidation, as shown in Figure 3. Afterwards, another layer of coverall powder was applied to the surface of the melt to continue protecting it from oxidation and to assist in removing slag.

The molten mixture was stirred thoroughly to ensure a uniform composition, and it was then quickly poured into a preheated grey cast iron mould (shown in Figure 4), which had been coated with graphite powder on the inner walls and heated to 200°C. The resulting cast, shaped into fingers of 170mm x 18mm diameter, was then quenched in water to enhance the grain structure of the composite material.

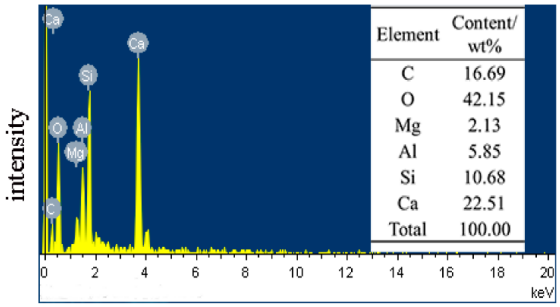

Fig. 2 Energy dispersive spectroscopy graphs for BF Slag

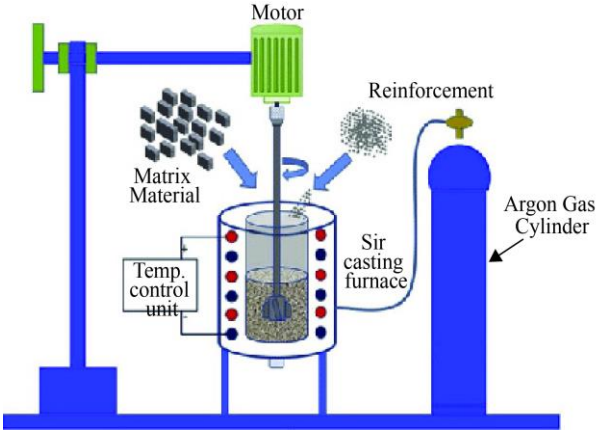

Fig. 3 Schematic diagram of stir casting with argon gas

Fig. 4 Grey cast iron mould

The fabrication procedure of binary alloy was depicted through a timeline chart in Figure 5.

Details of the process:

Melt Temperature of Al	: 700°C
Time of hold for melting	: 120 min
Mg addition and lurching	: 120 min for 2 min
Degassing agent	: Coverall
Degassing time	: 1 min
Mould material	: Grey cast iron
Mould dimensions	: 170mm x 18mm Φ
Mould pre-heated	: 200°C
Inert medium	: Argon gas

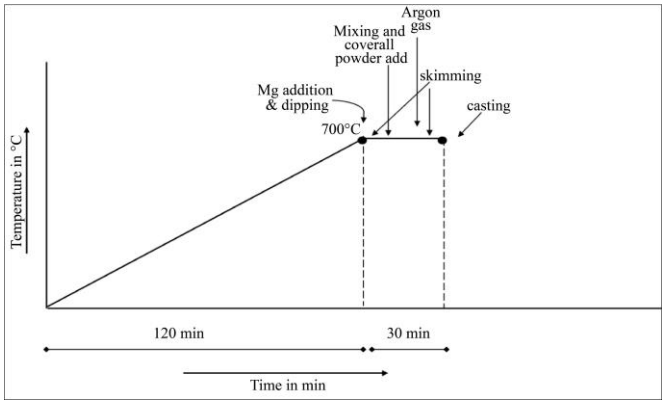

Fig. 5 Step-by-step procedure chart for preparation of Al-4Mg

Fig. 6 Cast fingers of the base alloy Al-4Mg

Table 2. Chemical composition of base alloy Al-4Mg in Wt%

Element	Si	Fe	Ti	Zn	Mn	Mg	Al
Wt.%	0.1	< 0.1	< 0.1	< 0.1	< 0.1	3.94	balance

2.3. Fabrication of Composites

The composites were manufactured using the stir casting method, where different weight percentages ranging from 5% to 10% were quickly and continuously added into the vortex created by stirring with a graphite impeller, which was electronically regulated, as depicted in Figure 7. The composites were reinforced with blast furnace slag particles, averaging 53 microns in size. They were then poured into a cast iron mold measuring 170 mm by 18 mm. To eliminate internal stresses, the composite materials underwent a complete homogenization process at 100°C for 24 hours.

2.4. Porosity Measurements

Measurements for both theoretically and experimentally reinforced and unreinforced composites were made in terms of porosity and density. The Rule of Mixtures approach was taken to carry out the theoretical measurement. An experimental measurement involved the use of Archimedes' law, which states that a body immersed in a fluid exerts an upward force equal to the weight of the fluid displaced.

Percentage of porosity = 1 x 100 (measured density / theoretical density) (1)

2.5. Microstructural Analysis

Microstructure evaluation was done on reinforced and un-reinforced composites to examine the grain refinement and uniform distribution of particles. The prepared samples were polished by using polishing papers to get a mirror surface. Etchant was used (10ml distilled water, 70ml of 95% ethanol, 4.2g Kellers agent 10ml acetic acid) in all samples to remove dirt on the surface.

2.6. Characterization of Composites

Composites with different volumes for 5 and 10 % reinforcement have been considered. As MMC was analyzed for the impact of reinforcement, conducting Vickers microhardness tests was inevitable. Results of Vickers microhardness test at a load of 100 gm and dwell time of 10s have been calculated as. For tensile strength and Young's modulus testing, the tensile tests were carried out on an Instron 8801 UTM calibrated at room temperature with a ram speed of 3 mm/min. The three samples taken into consideration for each case complied with the standards of ASTM E 8 and had been taken for tensile tests by conducting the tensile test on an average of three specimens.

3. Results and Discussions

3.1. Microstructure and Characterization

Figure 8(a): The microstructure of Al-4Mg base alloy with uniform distribution of the IDR is observed for the formation of a secondary phase or β-phase. From the micrograph of the composite with 5% reinforcement in Figure 8(b), a clear, uniform distribution of phase and consistency of growth of a dendrite is confirmed, which leads to the highest elongation comparatively and, hence, has the highest ductility. Figure 8(c) SEM micrograph of the composite with 10 % reinforcement shows clear enhanced grain refinement but no uniformity in the distribution of grains throughout. Thus this composite exhibited lesser tensile strength compared to composite with 5 % reinforcement. The reason for the decrease in properties at 10 % is due to agglomerations of the phases, which leads to failure of the material at lower strength. Main reasons for agglomeration in composite with 10% reinforcement the saturation of solubility of the powder particulate in the vortex of the base alloy leads to non-uniform mixing of particulate. The high volume of powder leads to a lowering of rotation of the stirrer in the vortex. Another factor that contributes to agglomeration is because of the time lag of mixing powder particulate in the melt of the base alloy. As the time lag increases, so does the lagging in the drop of the temperature of the melt of the alloy, as well as a lag in attaining uniformity in the phases. The reinforcement increment enhanced the composite properties.

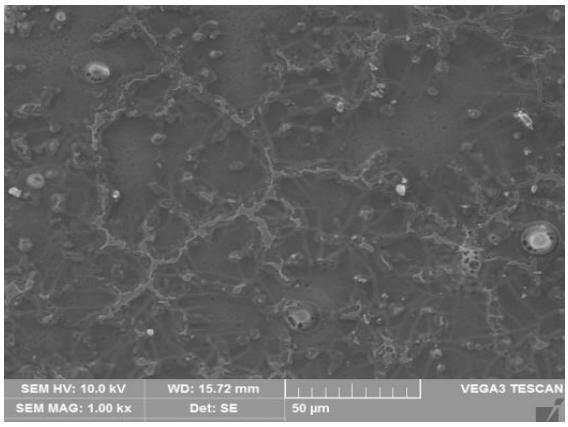

Fig. 8(a) SEM image for Al-4Mg alloy

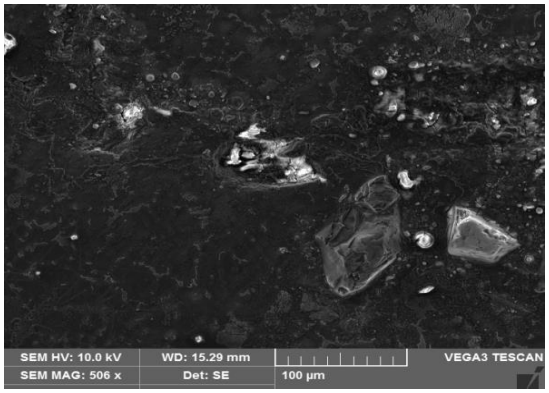

Fig. 8(b) SEM image of 5% composite

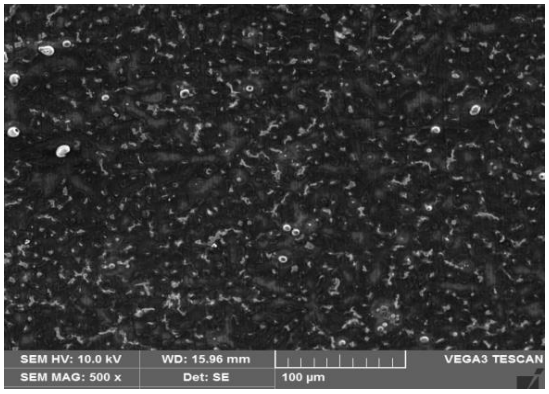

Fig. 8(c) SEM image of 10 % composite

3.2. Density and Porosity

Table 3 shows the Measured and theoretical density comparison. Low porosity results are achievable, as evidenced by successful castings, for the measured densities were still smaller than the theoretical density due to agglomeration, interstitial spaces, and a lack of continuity during stirring and casting that would have resulted in increased porosities from the reinforcements themselves. Both levels of porosities for composites were found to be low in comparison to the alloy, which speaks to the quality of the casting [18].

Table 3. Density and porosity of alloy and composites

S.NO.	Material	Density(g/cc) theoretical	Density(g/cc) Measured	% porosity
1	Al-4Mg	1.8	1.799	±0.6
2	5% C	1.82	1.812	±0.5
3	10% C	1.84	1.83	±0.62

3.3. Compression Strength

Due to an increase in BF Slag particles, the composites' compressive and yield strengths were raised. The composite's strength is influenced by the particle's size and the interfacial bonding of the reinforcement to the matrix [19]. The reduction in reinforcing particle size results in greater strength. When stress is applied, the interfacial adhesion between the reinforcement and the matrix is sufficient, and the magnesium alloy matrix may transition into the reinforced BF Slag particles.

Table 4. Compressive strength and yield strength

S. NO.	Material	Compressive Strength (MPa)	Compressive Strain mm/mm	Modulus of Elasticity (GPa)
1	Al-4Mg	173.42	0.324	2.4
2	5% C	313.35	0.281	2.7
3	10% C	380.20	0.132	2.6

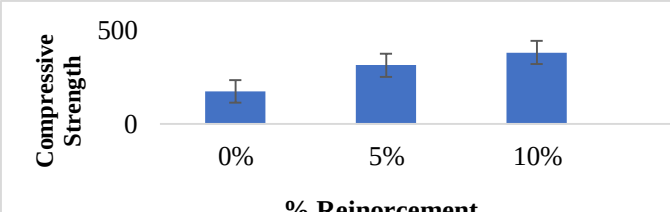

Fig. 9 Compressive strength of the composites

3.4. Tensile Strength

Tensile tests were conducted using an Instron testing machine for pre-calibration as done on the machine. Samples are prepared for test of the cross-section of the gauge length. The ultimate tensile strength of the composite is increased to 5% reinforcement, and tensile strength was found to decrease with the addition of 10% reinforcement. The processing variables such as holding temperature, stirring speed, size of the impeller and position of the impeller in the melt are important factors to be considered during cast of metal matrix composites [21]. The fractured specimens, which are loaded in tensile testing machines, are depicted in Figures 10(a) and 10 (b).

Table 5. Tensile test results

S. No.	Specimens	UTS MPa	Yield Stress	Modulus GPa
1	Al-4Mg	91.78	79.54	14.75
2	5% C	142.5	116.38	20.37
3	10 % C	106.8	90.51	17.75

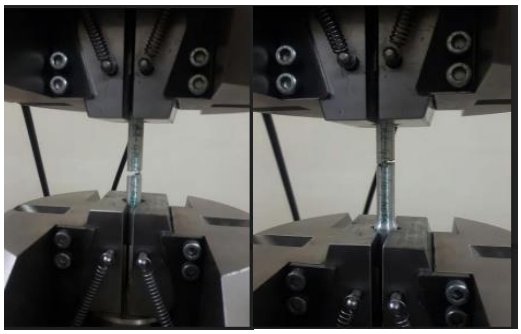

Fig. 10(a) & 10(b) Fractured specimens of AL-4Mg-5%&10% BFS composites

3.5. Hardness

Base alloy and composites were subjected to microhardness testing using a Leco Vickers hardness tester (Model LV700, USA) with an indentation time of 15s and 1kg load. Six readings were averaged. Ultimate tensile strength and compression measurements of the micro-alloyed composites were carried out using an Instron testing machine (Model 500KN UTM 8803J5353, UK), calibrated to ASTM-E8 standards, with an extensometer. As portrayed in Table 6, micro and macro hardness was observed to increase with an increase in percentage reinforcement in composite in comparison with the base alloy. This increase in hardness is due to the incorporation of blast furnace slag reinforcement particles distributed in the alloy matrix to increase its load-bearing capacity during indentation. The strong interfacial bonding between reinforcement particles and the matrix also accounts for the load transfer during indentation. Graphical variation in hardness values for alloy and composite Figure 11 shows. The pure alloy has a hardness value of 71.89 VHN. After the addition of 5% BF slag particles, the hardness value reads as 80.97 VHN, while the highest value of hardness is that of the composites with 10% BF slag reinforcement particles, for which the hardness value recorded was 90.08 VHN. The hardness of the composite increases due to the reinforcement particles as high strength and load-bearing capacity resist indentation during hardness testing. An increase in hardness values with an increase in the percent of reinforcement is due to the efficient distribution of reinforcement particles in the alloy matrix along with strong interfacial bonding, which establishes the transfer mechanism under indentation.

Table 6. Hardness value (VHN)

S. No.	Material	Micro Hardness
1	Al-4Mg Alloy	71.89
2	5% Composite	80.97
3	10% Composite	90.08

Figures 12(a), (b), (c), and (d) show the microstructure analysis and failure modes evidence for tensile test specimens. With an increased number of reinforcements within the same time constraint, there could be a non-uniform distribution of particles in the melt due to decreased wettability of the melt. This non-uniform distribution might be one of the reasons for the reduction in strength highlighted in the 10 wt. % composite. The elastic modulus E of a material, is stiffness in the elastic region and therefore higher in the 10 wt. % composite within this region. The Ultimate Tensile Strength (UTS) is the maximum load that a material can carry before the development of a neck. Between the three composites, the one with 5 wt. % reinforcement bears load better. Though the specific strength rises with an increase in the percentage of reinforcement from 5 to 10%, it is found that the ductility decreases largely because of cluster formation, which causes porosity.

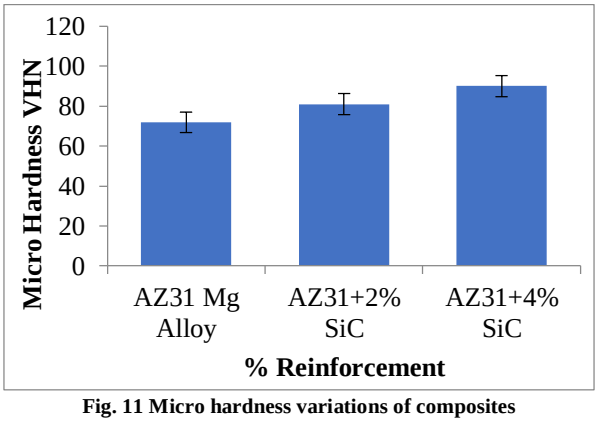

Fig. 11 Micro hardness variations of composites

3.6. Fractography

Figure 10 shows the tensile failure pattern of the specimens and the percentage of elongation indicating material ductility. Composite with a reinforcement of 5 wt. % is of a high ductile nature due to more grain refinement. Figure 12(a) the dimple structure of base alloy Al-4Mg. Figures 12(b) and 12(c) have agglomerations of the particulates which occurred in the composite with 10 wt. % reinforcement. Slag particles got pulled out from the base matrix, due to which tensile strength could be very less in this composite. Tear ridges are formed, as indicated in Figure 12(d).

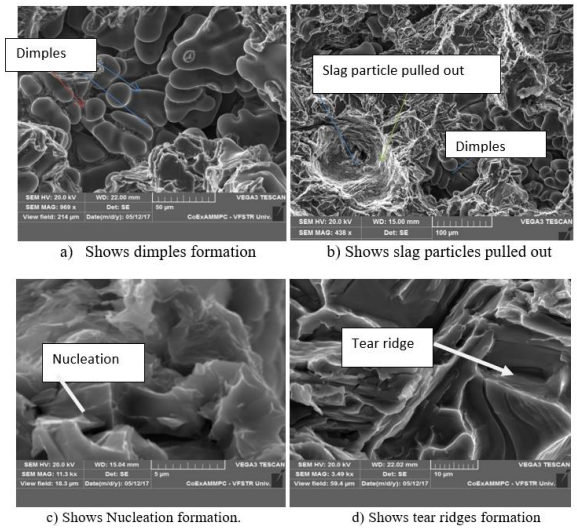

a) Shows dimples formation b) Shows slag particles pulled out

c) Shows Nucleation formation. d) Shows tear ridges formation

Fig. 12 SEM structure of failure of tensile specimens for 5%wt. and 10%wt of composites

3.7. TEM Analysis

Under certain conditions, the Al-Mg phase can also be precipitated in the melt itself at the eutectic point through rapid solidification or by the precipitation of a strong solution. The strength of the composite can be investigated through electron microscopic techniques, and through HRTEM analysis, the contribution of interfacial energies as well as other internal parameters, such as elastic constants, might become apparent. Figure 13(a-b) shows the TEM micrograph of the base alloy together with the SAED pattern depicting the grain boundary along which many dislocations have accumulated. In the TEM image of 5% reinforcement particulate, there is the occurrence of binary grain boundary Al-Mg with higher accumulated dislocation and very small and fine precipitate particles at boundaries.

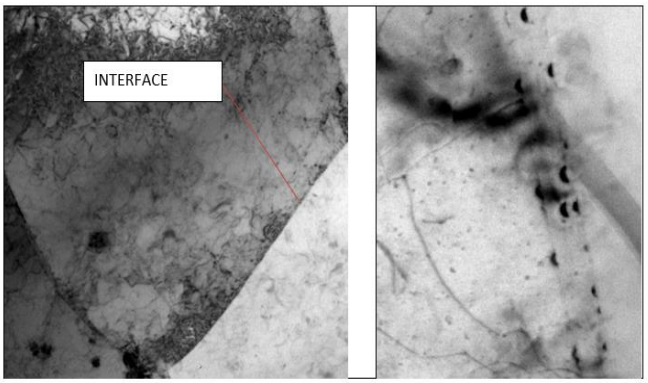

Fig. 13 (a) and (b) are the TEM micrographs of composite with 5 wt.% reinforcement showing grain boundaries and dislocation arrests

4. Conclusion

The composites were fabricated using the stir casting method, which resulted in a uniform distribution of particulates and bonding, as confirmed by microstructure analysis.

- The Vickers microhardness testing showed that the hardness value of the base alloy was 71.89 VHN. In comparison, the composites with 5% and 10% weight fractions of BF slag particles exhibited higher hardness values of 80.97 VHN and 90.08 VHN, respectively.
- The presence of slag particles in the matrix increased the compressive strength significantly, with the alloy exhibiting a compressive strength of 173.42 MPa, the composite with 5% reinforcement showing an increased compressive strength of 313.35 MPa, and the composite with 10% reinforcement exhibiting the highest compressive strength of 380.20 MPa. The Young's Modulus and ultimate tensile strength were also increased due to the presence of slag particles.
- The ultimate tensile strength of the composite with 5% reinforcement increased by 35% compared to the base alloy, while there was a 14% drop for the composite with 10% reinforcement. This decrease in tensile strength at higher reinforcement percentages may be due to the poor distribution of reinforcement particles in the melt, which reduces the wettability of the melt and leads to the agglomeration of particles.
- The use of slag particles in the composites resulted in a distinguished grain refinement, which further improved the mechanical properties of the composites.

References

[1] E. Aghion et al., "The Environmental Impact of New Magnesium Alloys on the Transportation Industry," *Magnesium Technology*, pp. 167-172, 2004. [Google Scholar] [Publisher Link]

[2] María Josefa Freiría Gándara, "Recent Growing Demand for Magnesium in the Automotive Industry," *Materials and Technology*, vol. 45, no. 6, pp. 633-637, 2011. [Google Scholar] [Publisher Link]

[3] Mustafa Kemal Kulekci, "Magnesium and its Alloys Applications in Automotive Industry," *The International Journal of Advanced Manufacturing Technology*, vol. 39, pp. 851-865, 2008. [CrossRef] [Google Scholar] [Publisher Link]

[4] D. Sameer Kumar et al., "Magnesium and Its Alloys in Automotive Applications– A Review," *American Journal of Materials Science and Technology*, vol. 4, no. 1 pp. 12-30. 2015. [Google Scholar]

[5] S. Jayalakshmi, S.V. Kailas, and S. Seshan, "Tensile Behaviour of Squeeze Cast AM100 Magnesium Alloy and its Al_2O_3 Fibre Reinforced Composites," *Composites Part A: Applied Science and Manufacturing*, vol. 33, no. 8, pp. 1135-1140, 2002. [CrossRef] [Google Scholar] [Publisher Link]

[6] A. Srinivasan et al., "Creep Behavior of AZ91 Magnesium Alloy," *Procedia Engineering*, vol. 55, pp. 109-113, 2013. [CrossRef] [Google Scholar] [Publisher Link]

[7] D.J. Lloyd, "Particle Reinforced Aluminium and Magnesium Matrix Composites," *International Materials Reviews*, vol. 39, no. 1, pp. 1-23, 1994. [CrossRef] [Google Scholar] [Publisher Link]

[8] S. Aravindan, P.V. Rao, and K. Ponappa, "Evaluation of Physical and Mechanical Properties of AZ91D/SiC Composites by Two Step Stir Casting Process," *Journal of Magnesium and Alloys*, vol. 3, no. 1, pp. 52-62, 2015. [CrossRef] [Google Scholar] [Publisher Link]

[9] Palash Poddar et al., "Processing and Mechanical Properties of SiC Reinforced Cast Magnesium Matrix Composites by Stir Casting Process," *Materials Science and Engineering: A*, vol. 460-461, pp. 357-364, 2007. [CrossRef] [Google Scholar] [Publisher Link]

[10] S.F. Hassan, and M. Gupta, "Enhancing Physical and Mechanical Properties of Mg using Nanosized Al_2O_3 Particulates as Reinforcement," *Metallurgical and Materials Transactions A*, vol. 36, pp. 2253-2258, 2005. [CrossRef] [Google Scholar] [Publisher Link]

[11] Manoj Gupta, and Wai Leong Eugene Wong, *An Insight Into Processing and Characteristics of Magnesium-Based Composites*, Magnesium Technology 2014, pp. 423-428, 2014. [CrossRef] [Google Scholar] [Publisher Link]

[12] J. Hashim, L. Looney, and M.S.J. Hashmi, "Metal Matrix Composites, Production by the Stir Casting Method," *Journal of Materials Processing Technology*, vol. 92-93, pp. 1-7, 1999. [CrossRef] [Google Scholar] [Publisher Link]

[13] S. Shankar, and S. Elango, "Dry Sliding Wear Behavior of Palmyra Shell Ash Reinforced Aluminium Matrix (AlSi10Mg) Composites," *Tribology Transactions*, vol. 60, no. 3, pp. 469-478, 2017. [CrossRef] [Google Scholar] [Publisher Link]

[14] A.M. Usman et al., "A Comparative Study on the Properties of Al-7% Si-Rice Husk Ash and Al-7% Si-Bagasse Ash Composites Produced by Stir Casting," *The International Journal Of Engineering And Science*, vol. 3, no. 8, pp. 1-7, 2014. [Google Scholar] [Publisher Link]

[15] Ch. Hima Gireesh et al., "Mechanical Characterization of Aluminium Metal Matrix Composite Reinforced with Aloe Vera Powder," *Materials Today: Proceeding*, vol. 5, no. 2, pp. 3289-3297, 2018. [CrossRef] [Google Scholar] [Publisher Link]

[16] B. Geetha, and K. Ganesan, "Optimization of Tensile Characteristics of Al 356 Alloy Reinforced with Volume Fraction of Red Mud Metal Matrix Composite," *Procedia Engineering*, vol. 97, pp. 614-624, 2014. [CrossRef] [Google Scholar] [Publisher Link]

[17] P. Poddar, S. Mukherjee, and K.L. Sahoo, "The Microstructure and Mechanical Properties of SiC Reinforced Magnesium Based Composites by Rheocasting Process," *Journal of Materials Engineering and Performance*, vol. 18, pp. 849-855, 2009. [CrossRef] [Google Scholar] [Publisher Link]

[18] Riccardo Casati, and Maurizio Vedani, "Metal Matrix Composites Reinforced by Nano-Particles-A Review," *Metals*, vol. 4, no. 1, pp. 65-83, 2014. [CrossRef] [Google Scholar] [Publisher Link]

[19] V. Mohanavel, and S. Suresh Kumar, "Mechanical Behavior of Al-Matrix Nanocomposites Produced by Stir Casting Technique," *Materials Today: Proceeding*, vol. 5, no. 13, pp. 26873-26877, 2016. [CrossRef] [Google Scholar] [Publisher Link]

[20] B. Praveen Kumar, and Anil Kumar Birru, "Microstructure and Mechanical Properties of Aluminium Metal Matrix Composites with Addition of Bamboo Leaf Ash by Stir Casting Method," *Transactions of Nonferrous Metals Society of China*, vol. 27, no. 12, pp. 2555-2572, 2017. [CrossRef] [Google Scholar] [Publisher Link]

[21] S. Suresh Kumar et al., "Physical and Mechanical Properties of Various Metal Matrix Composites: A Review," *Materials Today: Proceedings*, vol. 50, pp. 1022-1031, 2022. [CrossRef] [Google Scholar] [Publisher Link]

[22] A. Seshappa, K. Prudhvi Raj, and B. Anjaneya Prasad, "Fabrication and Characterization of Aluminium Hybrid Metal Matrix Composite with Power Chillers," *Materials Today: Proceddings*, vol. 46, no.1, pp. 786-789, 2021. [CrossRef] [Google Scholar] [Publisher Link]